Optical Materials: X 15 (2022) 100179

Contents lists available at ScienceDirect

Optical Materials: X

journal homepage: www.journals.elsevier.com/optical-materials-x

(INVITED)Tm:YAG crystal-derived double-clad fibers – A hybrid approach towards high gain and high efficiency Tm lasers

Martin Leich *, Robert Müller, Sonja Unger, Anka Schwuchow, Jan Dellith, Adrian Lorenz, Jens Kobelke, Matthias Jäger

Leibniz Institute of Photonic Technology, Albert-Einstein-Str. 9, Jena, 07745, Germany

ARTICLE INFO

Keywords:
Tm-doped fiber
Double-clad fiber
Fiber laser
Molten Core Method

ABSTRACT

The hybrid approach of combining a Tm:YAG laser crystal with an amorphous fused silica tube is investigated to evaluate the suitability of the resulting crystal-derived fibers for efficient double-clad fiber lasers. The fabrication process and fiber properties of these Tm fibers are investigated, focusing on the dependence of the active fiber properties on the incorporated Tm^{3+} concentration. Crystal rods with different doping concentrations $(Tm_xY_{1-x})_3Al_5O_{12}$ (x = 0.02, 0.05 and 0.08) were used as starting core material for fiber drawing. The investigated fibers are mechanically stable and result in a fairly homogenous and amorphous core glass with optical absorption and emission spectra that are similar to conventional Tm:Al doped silica fibers. Regarding laser properties with 790 nm cladding pumping, we could achieve a maximum slope efficiency of 47% with an output power of 4 W. The fiber laser results are compared to a conventionally fabricated double-clad Tm fiber prepared by Modified Chemical Vapor Deposition and solution doping. To the best of our knowledge, we demonstrate the highest laser output and the highest efficiency obtained from a Tm:YAG crystal-derived fiber.

1. Introduction

Fiber lasers have become increasingly popular in the recent two decades due to numerous advantages with respect to other solid state lasers, e.g. their robustness, efficient cooling, high power compatibility, flexibility, large gain bandwidth and easy handling. Some important applications, especially for the NIR range are material processing, medical applications, metrology and optical sensing.

In order to expand the areas of application, there is a great interest in new active materials that allow higher doping levels, e.g. for shortening the laser cavity length and therefore reducing nonlinear effects or pulse broadening for ultrashort pulsed lasers. Another big goal is the exploitation of new emission wavelength regions.

One promising approach to implement new materials into silica fibers, which are best established for the integration in optical fiber systems, is the Molten Core Method (MCM) introduced by Snitzer and Tumminelli [1] and reviewed comprehensively by J. Ballato and A. Peacock [2]. With this method multiple materials can be put into a glass tube in order to be drawn into fiber. One possibility to implement high doping levels of rare earths and Al ions is the use of rare-earth-doped YAG crystals.

Tm:YAG crystals as core material are of big interest when addressing the long NIR range around 2 μm wavelength, which is especially interesting for medical applications, e.g. tissue ablation [3], atmospheric spectroscopy [4] as well as for laser processing of plastics [5]. For efficient lasing, high doping concentrations of Tm and Al are required to enable the cross-relaxation (also known as 2-for-1 process) [6,7]. Efficiencies of >70% are possible depending on the fiber composition and quality. In Refs. [6,8] it is reported that an Al^{3+}/Tm^{3+} ratio of at least 10:1 is required for an efficient cross-relaxation process. This ratio in context with the required high Tm concentration of the laser core, the doping levels achievable with standard MCVD (Modified Chemical Vapor Deposition) and solution doping preform fabrication routes are quickly reaching the limit.

One essential challenge when drawing crystal rods in a silica tube is to find suitable drawing parameters that allow fiber fabrication with homogenous cores without scattering defects. The diffusion of silica into the molten core material is a very sensitive effect [9], and will mainly influence important fiber parameters, e.g. fiber loss and doping concentrations.

Several research groups have reported on fibers lasers with cores derived from crystals like Yb:YAG [10–12], but also on properties and

* Corresponding author.
E-mail address: martin.leich@leibniz-ipht.de (M. Leich).

https://doi.org/10.1016/j.omx.2022.100179
Received 15 July 2022; Received in revised form 19 August 2022; Accepted 21 August 2022
Available online 31 August 2022

design issues e.g. to pretend clustering of Er:YAG fibers [13,14]. In a few papers it is also reported on Tm:YAG [15,16] ceramic-derived fibers for ultrashort-pulse operation at low power and efficiencies up to 16.5%. To date, mainly crystal-derived single-clad fibers have been reported and hardly any double-clad fibers, with the exception of a work from Xie et al. on an all-fiber cladding-pumped Yb:YAG laser, where 6 W output power at 21.7% efficiency were demonstrated [11]. The approach to combine rare-earth-doped YAG crystals with silica tubes turned out to be very promising. YAG crystals are well-suited for MCM drawing in silica tubes because of their high melting temperature of 1950 °C lying in the range of typical drawing temperature of high purity silica glass, e.g. the well-established Heraeus F300 fused silica. The high refractive index of 1.83 @633 nm is lying well above the index of F300 silica glass (1.457) ensuring optical guidance of the fiber structure. One critical parameter is the diffusion that takes place between the silica tube and the crystal core material during fiber drawing. In general, diffusion results in more than 70% silica in the fiber core regarding 125 μm fibers with core to clad ratio of 1:10 of the preform [10–13,15].

In this work, we present the fabrication of three different preforms and fibers from silica tubes and differently doped Tm:YAG crystal rods using the MCM method. For the first time of our knowledge these fibers have a double-clad structure allowing high power cladding pumping. We show essential optical results and demonstrate very efficient laser operation of these fibers.

2. Methods

Crystal-derived fibers were fabricated by drawing Tm:YAG doped crystal rods in fused silica tubes following the Molten Core Method [1,2]. A reference fiber for comparison has been fabricated by Modified Chemical Vapor Deposition and solution doping [17].

Spectral attenuation of the fibers was measured by cut-back method [18] using different lengths of the fibers and a Spectro 320D fiber spectrometer by Instrument Systems. The stoichiometry of the fiber core region was investigated by wavelength-dispersive electron probe microanalysis (WD-EPMA, JXA-8800 L, JEOL, Japan). For that, we have initially performed high resolution line profiles across the whole fiber diameter for the elements in question using a highly focused electron beam and a step interval of the specimen stage of 500 nm. These line profiles were subsequently scaled with the results of fully quantitative spot analyses. The energy of the exciting electrons, E0, was set to 25 keV in all cases.

The detection of crystalline phases was examined using X-ray diffraction (XRD, device X'pert Pro, Malvern Panalytical, Almelo, The Netherlands, using CuKα radiation). For the investigations, about 2 m of fiber were decoated and ground in a mortar i.e. the investigated material contains fiber core and cladding. The latter one (SiO_2) of our fibers is always amorphous. The mean size of the crystallites was calculated from measurements of the XRD line width using the Scherrer formula.

3. Experimental and results

3.1. Preform preparation and fiber drawing

As first step, a Heraeus F300 silica tube with 30 mm × 3 mm (outer x inner diameter) dimension was grinded and polished in-house with double-D-shape to realize a suitable geometry for cladding pumping. The tube was further prepared for fiber drawing and for applying a certain pressure during the drawing process. As core material for the MCM method we decided for three differently Tm-doped YAG crystals $(Tm_xY_{1-x})_3Al_5O_{12}$ with x = 0.02, 0.05 and 0.08 according to the supplier and corresponding to 0.75, 1.875 and 3.0 mol% of the thulium oxides in the pure garnet. These crystal rods were delivered by Crytur, spol. s r.o. The high melting temperature of YAG allows drawing in high purity silica tubes, but drawing temperature must be carefully chosen to ensure a homogenous fiber core and to avoid deformation of the core and cladding structure. For each of the three crystal rods with length about 60 mm and 2.5 mm outer diameter a separate part of the preform tube was prepared for drawing: starting with a silica "dummy" rod (clear) inserted within the tube, being followed by the crystal rod (opaque section in Fig. 1). Both rods were inserted without pre-collapse. This procedure allows careful adjustment of the drawing parameters and fiber diameter before the crystal starts melting and possibly causing diameter fluctuations due to its very low viscosity.

All preforms have been drawn to fibers with similar outer diameter of 130 μm.136 μm. As can be seen from the microscopic images of the fiber cross-sections in Fig. 2, core size and shape are varying for each fiber. The reason can be slight variations in drawing temperature and speed. Fiber 2 shows an asymmetric core. This can be caused by the double-D shape of the preform, which is slightly more rounded than for the other two fibers.

The stoichiometric profiles of the fiber core region taken by WD-EPMA and depicted in Fig. 3 show parabolic-like diffusion profiles for all three fibers. Furthermore, marked in the profiles as thick horizontal lines are quantitative WD-EPMA results of fiber pieces of the opposite end of the drawn fiber (Pos2) having a slightly different stoichiometry, which indicates the changing fiber properties during the drawing process as it has also been reported for Er:YAG derived fibers in Ref. [14].

According to investigations of the system Y_2O_3–Al_2O_3–SiO_2 [18] an amount of at least 20 wt% SiO_2 (corresponding to about 35 mol% SiO_2 in the system Y_2O_3–Al_2O_3–SiO_2) is necessary for glass formation in samples quenched with about 200 K/s. Despite of higher SiO_2-contents in the fiber cores and an assumed faster quenching during fiber drawing we investigated the possible formation of crystalline phases by X-ray diffraction (described in chapter 2).

Fig. 4(left) shows the XRD patterns of the fibers, all dominated by amorphous material. In fiber 3, α-Al_2O_3 could be detected (indicated by *) with a crystallite size of about 200 nm. As well, one peak not fitting to the α-Al_2O_3 pattern was detected that might belong to a SiO_2 phase. In fiber 2, only three tiny diffraction peaks are visible without doubt that did not allow a determination of the crystalline phase. However, α-Al_2O_3 can be excluded. The crystallinity (volume fraction) estimated from peak areas is below 0.1%. In fiber 1, there might be an indication of one peak, however it is doubtful.

Additionally, core attenuation of all fibers was measured with core-size matched coupling and collection fibers to avoid influence of guided cladding light by cut-back method [19]. In Fig. 4(right), the loss spectrum of the original Tm:YAG crystal and corresponding fiber 1 are depicted. Typical narrow absorption lines for the YAG crystal (grey curve) disappear after fiber drawing and result in broad absorption

Fig. 1. Preform prepared for drawing (rod-in-tube method) with silica rod for drawing process start-up phase followed by Tm:YAG crystal.

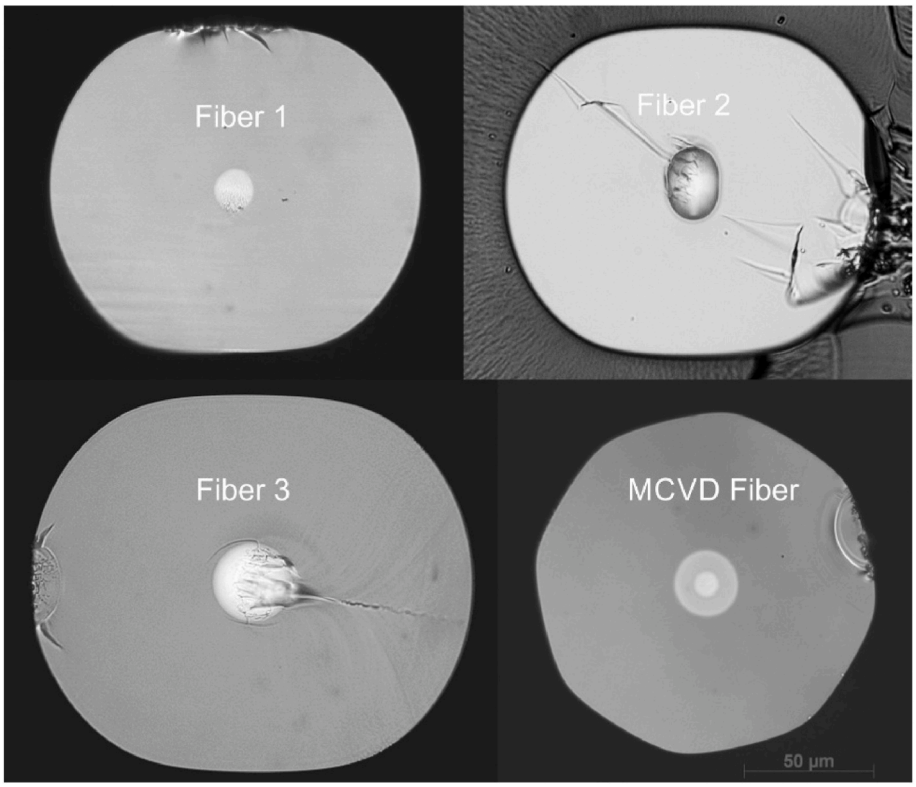

Fig. 2. Cross-sections of crystal-derived fibers with different crystal rods and Tm-doped MCVD fiber.

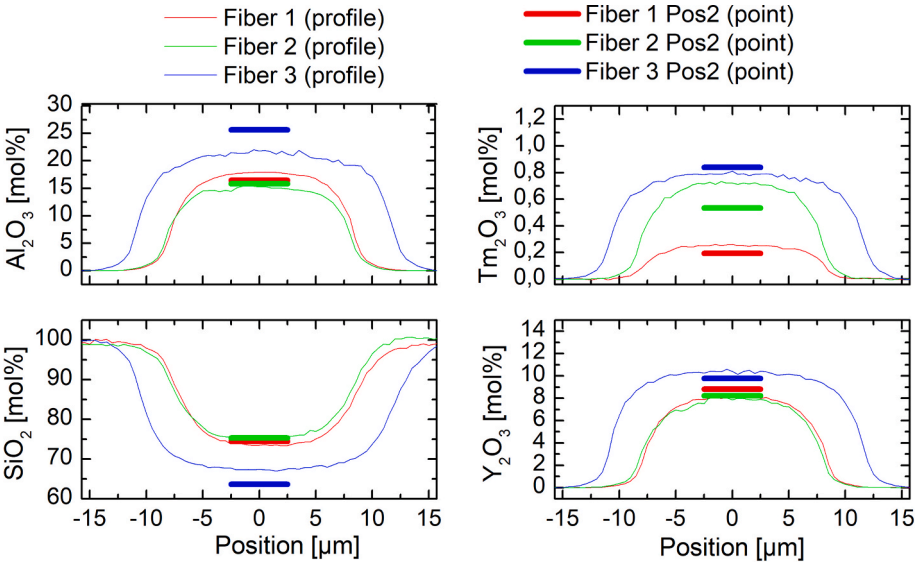

Fig. 3. EPMA measurements showing profile (thin lines) and quantitative point measurements at different fiber position (thick lines).

peaks (red curve), further indicating that the resulting fiber tends strongly towards an amorphous SiO_2–Al_2O_3–Y_2O_3 glass.

As a reference to evaluate the quality and laser performance of the crystal-derived fibers (CDFs), an in-house Tm double-clad fiber (Table 1, MCVD fiber) was fabricated by MCVD and solution doping with similar Tm^{3+} concentration as fiber 2, codoped with Al and a low amount of P (0.5 mol% P_2O_5). This fiber is a single-mode fiber with Ge-doped pedestal and octagonal cladding cross-section. For all drawn fibers, important parameters are listed in Table 1.

3.2. Fiber laser experiments

The laser performance of the Tm-doped crystal-derived fibers was investigated in an experimental setup for cladding-pumping and free-space pump coupling, which is depicted in Fig. 5. Pump light from a non-stabilized 790 nm fiber-coupled pump diode with 105 µm fiber core from DILAS is coupled into the cladding of the Tm-doped fiber, passing a butt-coupled dichroitic mirror, which is high transmissive for the pump and high reflective from 1700 to 2110 nm. This butt-coupled mirror at the perpendicular fiber front facet and a perpendicular end facet at the fiber back side are forming the laser resonator. Since cleaving of the

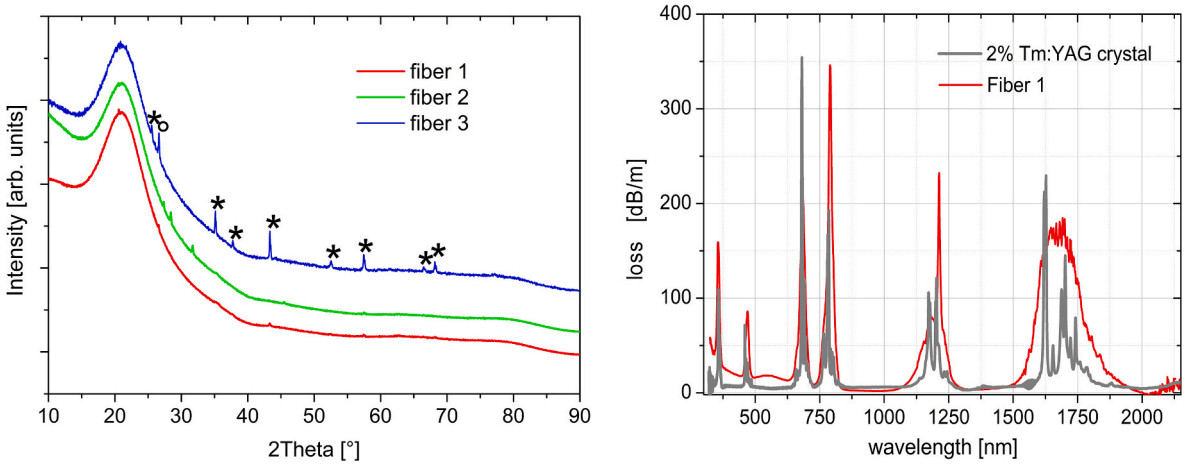

Fig. 4. Left: XRD pattern of crystal derived fibers. * indicates peaks fitting to Al_2O_3, **right**: loss spectrum of fiber 1 and corresponding Tm:YAG crystal.

Table 1
Parameters of crystal-derived fibers.

Fiber properties	Fiber 1	Fiber 2	Fiber 3	MCVD fiber
$d_{core/clad}$ [µm]	15 × 13.8/ 130	25 × 17.6/ 135	24/ 136	10/130
d_{core}/d_{clad}	0.11	0.14	0.18	0.077
Tm_2O_3 [mol%]	0.193	0.534	0.836	0.5
Y_2O_3 [mol%]	8.8	8.23	9.8	–
Al_2O_3 [mol%]	16.5	15.82	25.62	4.0
SiO_2 [mol%]	74.4	75.3	63.7	95
Ratio Tm:Al	1:85.5	1:29.6	1:30.6	1:8
Core attenuation at 950 nm [dB/m]	2	1.9	2.4	0.3

crystal-derived fiber is very difficult and stress-induced cracks in the core region cannot be avoided because of the extremely different thermal expansion coefficients of the YAG-derived core material and the silica cladding, fiber ends were polished.

In Fig. 6 (left), the laser output power is plotted versus the absorbed pump power, which was determined from the difference between the coupled and transmitted pump power for each fiber. The coupled pump power was determined at a 15 cm short piece of the low-doped Tm fiber 1 by measuring the pump transmission and correcting for pump absorption. The pump absorption was determined via cutback measurement at low pump powers (below laser threshold). The determined values for coupled pump power, which correlate with $P_c = 0.88{*}P_{diode}$ (with coupled pump power P_c and output power of the pump diode P_{diode}) were taken as reference for all 3 CDFs because of their similar cladding geometry and difficulty to perform this measurement at highly Tm-doped fibers.

For each fiber, the fiber length has been optimized to achieve maximum efficiency. From the depicted plots the laser slope efficiency is directly determined resulting in 32.6% for fiber 1, 47% for fiber 2, 29% for fiber 3 and 54% for the MCVD reference fiber.

According to the optimal fiber length determined, fiber 1 absorbs 79% of the pump light, while fiber 2 absorbs 92%, fiber 3 absorbs 88% and the MCVD fiber absorbs 99% of the pump light. These different lengths with regard to the fiber absorption length lead to the output spectra shown in Fig. 6 (right), which vary slightly around the transmission wavelength of 2 µm.

4. Discussion

All fabricated CDFs show high optical quality with background loss of 1.9 … 2.4 dB/m, which is within a typical range, but could be further decreased compared to literature. In the absorption spectra (Fig. 4), the spectral broadening indicates the amorphous nature of the fiber core. This is further supported by XRD measurements at the fiber material: Except for fiber 3 nearly no crystalline phase has been detected. In fiber 3, some α-Al_2O_3 crystallites have been detected that might be an indication for enhanced scattering on small particles or crystallites that have formed during fiber drawing and therefore being responsible for the slightly higher loss value (see Table 1) with respect to the other CDFs.

From fiber laser experiments it is obvious that fiber 2 shows the highest slope efficiency with 47% and output power of 4 W for the tested CDFs. The slope is only slightly lower than for the reference MCVD fiber with a similar Tm^{3+} concentration yielding a slope efficiency of 54%. This efficiency is well above the Stokes limit of 40% considering signal and pump wavelengths at 2000 nm and 790 nm, respectively and

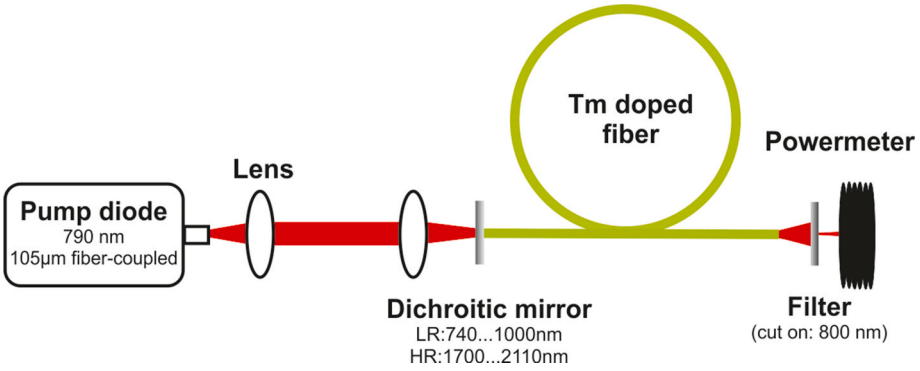

Fig. 5. Setup for fiber laser experiment.

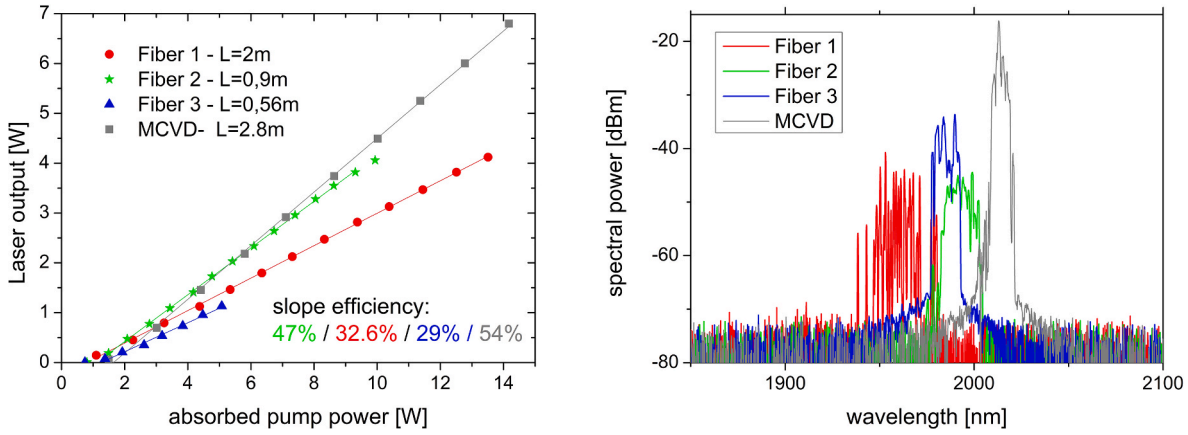

Fig. 6. Slope (left) and spectra (right) for crystal-derived and MCVD fibers.

therefore demonstrates an efficient cross-relaxation contribution. Fiber 1 and 3 are less efficient. For the former, the reason could lie in the relatively low Tm^{3+} concentration being below the threshold of efficient cross-relaxation [6]. For fiber 3, the low efficiency is not fully understood, but it could suffer from some inhomogeneity or scattering due to the measured formation of small crystallites during fiber drawing, which can also have an impact of the elements distribution and possible quenching effects in the glass. These observations show how sensitive the influence of fiber drawing parameters is on the properties of such MCFs. Further improvement of background loss and better control of diffusion parameters will help to further improve this new type of active fibers.

5. Conclusion

We have demonstrated successful drawing of crystal-derived double-clad fibers from three different crystal rods with varying in Tm-doping. The amorphous nature of the CDFs can be assumed from the spectral shape of the absorption spectra as well as the XRD results. For fiber 3, there are indications of crystallization after fiber drawing that can enhance scattering loss.

To the best of our knowledge, up to date we could demonstrate the highest output power of 4 W and the highest slope efficiency with 47% from a Tm-doped CDF. We also compared for the first time directly the laser properties of a CDF with a similarly Tm-doped MCVD fiber, which shows a slightly higher efficiency of 54%, but a remarkable lower background loss.

From the obtained results can be concluded that the MCM is a very promising technology to realize highly efficient, high gain laser fibers. Regarding Tm fibers, but not limited to this rare-earth, there is a big potential for developing very efficient short-cavity fiber lasers and amplifiers.

Funding

The project on which these results are based was supported by the Free State of Thuringia under the number 2018 FGR 0096 and co-financed by European Union funds within the framework of the European Social Fund (ESF).

CRediT authorship contribution statement

Martin Leich: Investigation, Writing – original draft, Visualization. **Robert Müller:** Writing – review & editing, Conceptualization, Investigation. **Sonja Unger:** Resources, Writing – review & editing, Validation. **Anka Schwuchow:** Resources, Investigation. **Jan Dellith:** Investigation, Writing – review & editing, Validation. **Adrian Lorenz:** Resources, Investigation, Writing – review & editing. **Jens Kobelke:** Resources, Investigation. **Matthias Jäger:** Conceptualization, Methodology, Writing – review & editing.

Declaration of competing interest

The authors declare that they have no known competing financial interests or personal relationships that could have appeared to influence the work reported in this paper.

Acknowledgments

We acknowledge Marco Diegel for performing the XRD measurements and Tina Eschrich for preparing fiber end facets by polishing and for her assistance in fiber characterization.

References

[1] E. Snitzer, R. Tumminelli, SiO2-clad fibers with selectively volatilized soft-glass cores, Opt. Lett. 14 (1989) 757–759, https://doi.org/10.1364/ol.14.000757.
[2] J. Ballato, A.C. Peacock, Perspective: molten core optical fiber fabrication-A route to new materials and applications, APL Photonics 3 (2018), 120903, https://doi.org/10.1063/1.5067337.
[3] Y. Huang, J. Jivraj, J. Zhou, J. Ramjist, R. Wong, X. Gu, V.X.D. Yang, Pulsed and CW adjustable 1942 nm single-mode all-fiber Tm-doped fiber laser system for surgical laser soft tissue ablation applications, Opt Express 24 (2016) 16674–16686, https://doi.org/10.1364/OE.24.016674.
[4] M. Tao, B. Tao, Z. Hu, G. Feng, X. Ye, J. Zhao, Development of a 2 μm Tm-doped fiber laser for hyperspectral absorption spectroscopy applications, Opt Express 25 (2017) 32386–32394, https://doi.org/10.1364/OE.25.032386.
[5] Y. Kurosakia, K. Satoh, A fiber laser welding of plastics assisted by transparent solid heat sink to prevent the surface thermal damages, LANE 2010, Phys. Procedia 5 (2010), https://doi.org/10.1016/j.phpro.2010.08.042, 173–18.
[6] S.D. Jackson, Cross relaxation and energy transfer upconversion processes relevant to the functioning of 2 μm Tm3+-doped silica fibre lasers, Opt Commun. 230 (2004) 197–203, https://doi.org/10.1016/j.optcom.2003.11.045.
[7] N.J. Ramírez-Martínez, M. Núñez-Velázquez, A.A. Umnikov, J.K. Sahu, Highly efficient thulium-doped high-power laser fibers fabricated by MCVD, Opt Express 27 (2019) 196–201, https://doi.org/10.1364/OE.27.000196.
[8] S. Jackson, S. Mossman, Efficiency dependence on the Tm3+ and Al3+ concentrations for Tm3+-doped silica double-clad fiber lasers, Appl. Opt. 42 (2003) 2702–2707, https://doi.org/10.1364/AO.42.002702.
[9] M. Cavillon, P. Dragic, B. Faugas, T.W. Hawkins, J. Ballato, Insights and aspects to the modeling of the molten core method for optical fiber fabrication, Materials 12 (2019) 2898, https://doi.org/10.3390/2Fma12182898.
[10] P.D. Dragic, J. Ballato, T. Hawkins, P. Foy, Feasibility study of Yb:YAG-derived silicate fibers with large Yb content as gain media, Opt. Mater. 34 (2012) 1294–1298, https://doi.org/10.1016/j.optmat.2012.02.019.
[11] Y. Xie, Z. Liu, Z. Cong, Z. Qin, S. Wang, Z. Jia, C. Li, G. Qin, X. Gao, X. Zhang, All-fiber-integrated Yb:YAG-derived silica fiber laser generating 6 W output power, Opt Express 27 (2019) 3791–3798, https://doi.org/10.1364/OE.27.003791.
[12] Z. Liu, Y. Xie, Z. Cong, Z. Zhao, Z. Jia, C. Li, G. Qin, S. Wang, X. Gao, X. Shao, X. Zhang, 110 mW single-frequency Yb:YAG crystal-derived silica fiber laser at 1064 nm, Opt. Lett. 44 (2019) 4307–4310, https://doi.org/10.1364/OL.44.004307.
[13] J. Ballato, T. Hawkins, P. Foy, B. Kokuoz, R. Stolen, C. McMillen, M. Daw, Z. Su, T. M. Tritt, M. Dubinskii, J. Zhang, T. Sanamyan, M.J. Matthewson, On the

fabrication of all-glass optical fibers from crystals, J. Appl. Phys. 105 (2009), 053110, https://doi.org/10.1063/1.3080135.
[14] A. Vonderhaar, M.P. Stone, J. Campbell, T.W. Hawkins, J. Ballato, P.D. Dragic, Concentration quenching and clustering effects in Er:YAG-derived all-glass optical fiber, Opt. Mater. Express 11 (2021) 3587–3599, https://doi.org/10.1364/OME.437825.
[15] Y. Zhang, G. Qian, X. Xiao, et al., The preparation of yttrium aluminosilicate (YAS) glass fiber with heavy doping of Tm3+ from polycrystalline YAG ceramics, J. Am. Ceram. Soc. 101 (2018) 4627–4633, https://doi.org/10.1111/jace.15722.
[16] G. Tang, G. Qian, W. Lin, W. Wang, Z. Shi, Y. Yang, N. Dai, Q. Qian, Z. Yang, Broadband 2 μm amplified spontaneous emission of Ho/Cr/Tm:YAG crystal derived all-glass fibers for mode-locked fiber laser applications, Opt. Lett. 44 (2019) 3290–3293, https://doi.org/10.1364/OL.44.003290.
[17] K. Schuster, S. Unger, C. Aichele, F. Lindner, S. Grimm, D. Litzkendorf, J. Kobelke, J. Bierlich, K. Wondraczek, H. Bartelt, Material and technology trends in fiber optics, Adv. Opt. Technol. 3 (2014) 447–468, https://doi.org/10.1515/aot-2014-0010.
[18] A. Schwuchow, S. Unger, S. Jetschke, J. Kirchhof, Advanced attenuation and fluorescence measurement methods in the investigation of photodarkening and related properties of ytterbium-doped fibers, Appl. Opt. 53 (2014) 1466–1473, https://doi.org/10.1364/AO.53.001466.
[19] R. Harrysson, P. Vomacka, glass formation in the system Y203-a1203-SiO2 under conditions of laser melting, J. Eur. Ceram. Soc. 14 (1994) 377–381, https://doi.org/10.1016/0955-2219(94)90075-2.